arXiv:1606.03703v1 [cond-mat.dis-nn] 12 Jun 2016

Fractional lattice charge transport

Sergej Flach[1,2], Ramaz Khomeriki[1,3],
[1] *Center for Theoretical Physics of Complex Systems, Institute for Basic Science, Daejeon, South Korea*
[2] *New Zealand Institute for Advanced Study, Centre for Theoretical Chemistry & Physics, Massey University, Auckland, New Zealand*
[3] *Physics Department, Tbilisi State University, Chavchavadze 3, 0128 Tbilisi, Georgia*

We consider the dynamics of noninteracting electrons on a square lattice in the presence of a magnetic flux α and a dc electric field E oriented along the lattice diagonal. In general, the adiabatic dynamics of an electron will be characterized by Bloch oscillations in the electrical field direction and dispersive ballistic transport in the perpendicular direction. For rational values of α and a corresponding discrete set of values of $E(\alpha)$ vanishing gaps in the spectrum induce a fractionalization of the charge in the perpendicular direction - while left movers are still performing dispersive ballistic transport, the complementary fraction of right movers is propagating in a dispersionless relativistic manner in the opposite direction. Generalizations to other field directions, lattice symmetries and the possible probing of the effect with atomic Bose-Einstein condensates and photonic networks are discussed.

PACS numbers: 67.85.-d, 37.10.Jk, 03.65.Ge, 03.65.Aa

The two-dimensional electron gas in a perpendicular magnetic field is a celebrated topic in condensed matter physics (see e.g. Ref. [1]). Electron-electron correlations or electron-lattice interactions lead to fractional quantum Hall physics, while the integer quantum Hall effect is based on the properties of the single particle eigenstates in the presence of a weak dc electric field in the linear response regime. Underlying discrete lattice structures and symmetries can have substantial impact on the wavefunctions. The well-known case of a two-dimensional square lattice leads to the much-studied Harper model [2] by reducing the two-dimensional problem to the dynamics in a one-dimensional quasi-periodic potential. Interestingly the interplay of the two-dimensional lattice structure with magnetic fields *and* a substantial in-plane electric field is far from being well understood, despite some notable publications [3, 4] and [5], where asymmetric spreading regimes have been observed for few different directions of the in-plane electric field with respect to the lattice axes [6].

While the generalized translational invariance - with shifts in space and energy - is preserved in the presence of an electric field, details do depend on the orientation. A field orientation along a main lattice axis is the most simple yet trivial case since the shift is identical with the lattice spacing. A general orientation angle of the electric field relative to the lattice axes will lead to potentially very large or possibly even infinite shifts. We investigate the nontrivial case with the electric field being oriented along the diagonal of the square lattice, which leads to a period doubling of the shifts. The band structure is in general given by infinitely many interconnected bands gapped away from each other. We show here that the gaps between the bands surprisingly vanish at particular values of the electric field. Treatable cases correspond to rational relative magnetic flux values. The resulting band structure is given by intersecting left and right mover bands with opposite average group velocities. Moreover, the unexpected outcome is that the right movers have a relativistic linear dispersion. Wavepackets of initially localized particles are then shown to split into two parts, with a fractional relativistic current of right movers. While experiments using a two-dimensional electron gas might be a challenging task, our results could

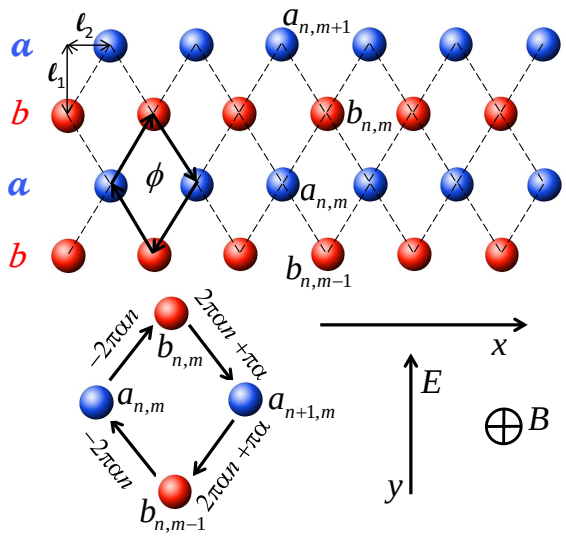

FIG. 1: Schematics for the square lattice with legs a (blue) and b (red). Dashed lines connect sites with allowed hopping/tunneling of the particle. The magnetic flux ϕ is induced by the perpendicular magnetic field B and traverses the elementary rhombus with half diagonals ℓ_1 and ℓ_2. The corresponding phases $\gamma_{ll'}$ are shown in the lower zoom of one plaquette, and the arrows indicate the direction of integration of (2). The dc electric field E is oriented along the y-axis. Therefore charge transport is observed along the x direction.

be directly verified in the context of Bose-Einstein condensates in optical lattices where the effective electric field is generated by a tilt of the lattice in the gravitational field [7] or accelerating a whole lattice [8], while the magnetic field is produced by artificial gauge fields [9]. Further, light propagation in waveguide networks can emulate the electric field analogy with a curved geometry of the waveguides [10], while a special metallic fabrication of the waveguides and the surrounding medium [11] leads to phase shifts of tunneling rates which leads to a magnetif field analogy.

We consider the following Hamiltonian describing single electron dynamics in a tight-binding lattice (see Fig. 1), in the presence of out-off plane magnetic $B \parallel z$ and in-plane electric $E \parallel y$ dc fields:

$$\hat{\mathcal{H}} = \sum_{\langle \ell\ell' \rangle} e^{i\gamma_{\ell\ell'}} \hat{q}_\ell^+ \hat{q}_{\ell'} + \sum_\ell \ell_y E \hat{q}_\ell^+ \hat{q}_\ell \, . \tag{1}$$

Here $\hat{q}_\ell^+$ and $\hat{q}_\ell$ are standard particle creation and annihilation operators at the ℓ-th lattice site. The voltage drop between neighbouring a, b chains is denoted by V. The first term in the Hamiltonian accounts for the hopping between nearest neighbor sites ℓ and ℓ' in the presence of a magnetic field. The corresponding phase factor is given [12]:

$$\gamma_{\ell\ell'} = \frac{2\pi e}{hc} \int_\ell^{\ell'} \vec{A} d\vec{s} \, . \tag{2}$$

The vector potential is defined in the Landau gauge as $\vec{A} \equiv (0, \; xB, \; 0)$. We denote the flux through the elementary rhombus (with diagonals $2\ell_1$ and $2\ell_2$) as $\phi = 2B\ell_1\ell_2$. With the flux quantum $\phi_0 = hc/e$, the relative flux is defined as $\alpha = \phi/\phi_0$. The voltage drop between a, b chains follows as $V = El_1$. The Schrödinger equation

$$i\partial\Psi/\partial t = \hat{\mathcal{H}}\Psi \tag{3}$$

describes the evolution of the particle wave function Ψ with time-dependent complex probability amplitudes $a_{n,m}$, $b_{n,m}$ assigned to all lattice sites. With the notations $c_{n,2m} = a_{n,m}$, $c_{n,2m+1} = b_{n,m}$, $\theta = 2\pi\alpha$ (flux angle) and the transformation

$$c_{n,l} = C_l e^{i(kn - \lambda t)} e^{-i\pi\alpha n(2l-1)} \tag{4}$$

which takes the space direction x (index n) transversal to the applied electrical field into Fourier space with wave number k, we arrive at a simple one-dimensional bipartite chain equation (see [13] for derivation details)

$$\begin{aligned} \lambda C_l = (l - \tfrac{1}{2})VC_l - [1 + e^{(-1)^l i(-k + l\theta)}]C_{l+1} \\ -[1 + e^{(-1)^l i(-k + (l-1)\theta)}]C_{l-1} \, . \end{aligned} \tag{5}$$

For each value of k the equation set (5) corresponds to a generalized Wannier-Stark ladder with a discrete unbounded spectrum $\lambda_\nu(k)$. Bands with different indices ν will generically avoid intersections upon varying the wave number k due to level repulsion [14]. As a result, an initially localized electron will be trapped and perform generalized Bloch oscillations in the y-direction. At the same time, on ballistic dispersive spreading will occur in the x-direction due to the overlap of the initial state with states from an effective finite number of bands. With $\partial^2\lambda_\nu(k)/\partial k^2 \neq 0$ the spreading will be dispersive in both x-directions, since a whole spectrum of group velocities will lead to a widening of the wave packet.

We do observe this outcome in general, however, we find that for each value of relative magnetic flux α a value of the electric field exists, for which a localized fraction of the wave packet is propagating in the *opposite direction* with a well defined velocity $V/(2\pi\alpha)$. We also observe that precisely for those parameter values the gaps in the above discussed band structure vanish (this can indeed happen for matrices with elements depending on more than one parameter [14]). In Fig. 2 the wave packet is shown for $\alpha = 1/3$ and $V = \sqrt{4.8}$ at different times. Indeed one third of the wave packet is propagating in a nondispersive localized manner to the right, while the complementary wave packet part is spreading as usual to the left (the wave packet dynamics is obtained by inte-

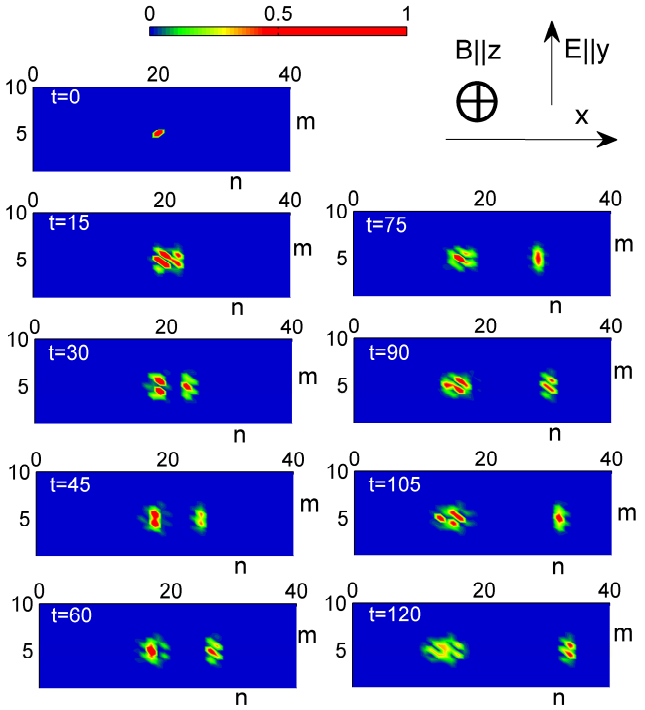

FIG. 2: The evolution of the wave packet ($|a_{n,m}|^2$ and $|b_{n,m}|^2$) of a single electron placed initially in the center of the two-dimensional lattice. Distributions for different times are presented. The right top graph shows the orientation of the dc electric and magnetic fields.

grating equation (3) in time).

Clearly the condition for the occurence of a charge fractionalization must be routed in the zeroing of gaps in the band structure, which lead to effective left- and right-movers. To proceed we investigate the matrix $\hat{M}$ whose zero determinant is yielding the eigenvalues λ of (5):

$$\hat{M} = \begin{pmatrix} \ddots & \vdots & \vdots & \vdots & \vdots & \vdots & \vdots & \vdots & \\ \cdots & 0 & -1-e^{i(k+2\theta)} & -\lambda-\frac{3V}{2} & -1-e^{i(k+\theta)} & 0 & 0 & 0 & 0 \cdots \\ \cdots & 0 & 0 & -1-e^{-i(k+\theta)} & -\lambda-\frac{V}{2} & -1-e^{ik} & 0 & 0 & 0 \cdots \\ \cdots & 0 & 0 & 0 & -1-e^{ik} & -\lambda+\frac{V}{2} & -1-e^{i(k-\theta)} & 0 & 0 \cdots \\ \cdots & 0 & 0 & 0 & 0 & -1-e^{-i(k-\theta)} & -\lambda+\frac{3V}{2} & -1-e^{-i(k-2\theta)} & 0 \cdots \\ & \vdots & \vdots & \vdots & \vdots & \vdots & \vdots & \vdots & \ddots \end{pmatrix} \quad (6)$$

The band structure $\lambda_\nu(k)$ follows from $Det[\hat{M}] = 0$. Matrix (6) is invariant under the symmetry operation

$$\lambda \to \lambda - V \ , \ k \to k + \theta \ . \quad (7)$$

Further, the spectrum $\lambda_\nu(k)$ is invariant under the symmetry operation

$$k \to -k \ , \ V \to -V \ . \quad (8)$$

It follows, that if the eigenenergy λ is degenerated for some values of the voltage V and wavenumber k, then the eigenenergy $\lambda' = \lambda - V$ exists and is also degenerated for the same voltage V at wavenumber $k' = k + \theta$. Therefore closing one gap in the spectrum implies closing all symmetry related gaps as well. For the particular case of $\lambda = 0$ and $k = \pi$ the matrix $\hat{M}$ splits into two semi-infinite blocks, and we then arrive at the general statement that gaps must close for particular values of pairs of θ and V (see [13] for details).

Rigorous results are obtained for rational values of α. In these cases the matrix $\hat{M}$ splits into noninteracting block matrices of finite size. Consider $\alpha = 1/3$. The band structure is shown in Fig.3(a-c) for various voltage drops. The matrix $\hat{M}$ splits into 3×3 block matrixes, with one of them given by

$$\hat{M}^{(3)} = \begin{pmatrix} \frac{V}{2} & 1-e^{-2i\pi/3} & 0 \\ 1-e^{2i\pi/3} & \frac{3V}{2} & 1-e^{4i\pi/3} \\ 0 & 1-e^{-4i\pi/3} & \frac{5V}{2} \end{pmatrix} . \quad (9)$$

The condition $Det\left(\hat{M}^{(3)}\right) = 0$ yields the roots $V = 0$ and $V = \pm\sqrt{4.8}$. It follows that for relative flux $\alpha = 1/3$ and voltage drop $V = \pm\sqrt{4.8}$ a nontrivial gap closing takes place which is indeed observed in Fig. 3 c). We then consider a particle initially localized on one site evolve this state in time according to (3). We compute the integrated charge density

$$Q_n = \sum_l |c_{n,l}|^2 \quad (10)$$

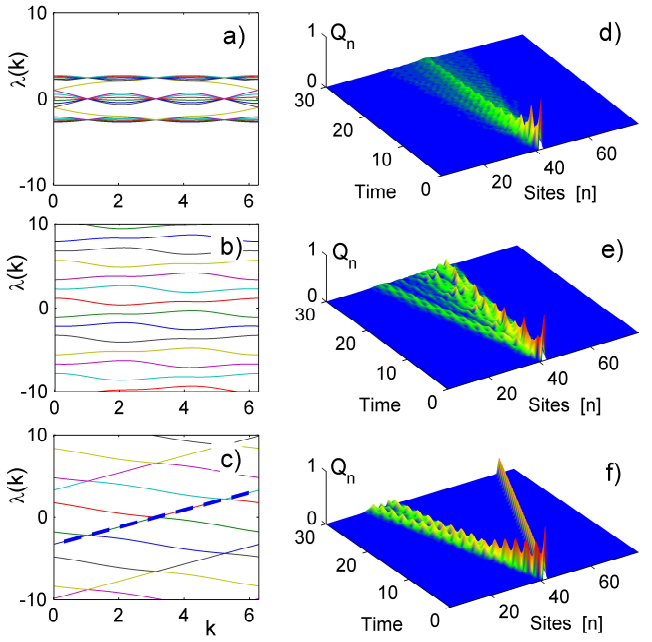

FIG. 3: Graphs a)-c): Dispersion relations for the Bloch bands after diagonalizing matrix (6) with dimensions 80×80.The relative flux is $\alpha = 1/3$ and the voltage drop take the values (from top to bottom) $V = 0$, $V = 1$ and $V = \sqrt{4.8}$. Graphs d)-f) show the wavepacket spreading upon integrating (3) with a single site initial condition using the parameters of the respective left panel graphs. The dynamics of the integrated charge density (10) accumulated in the n-th cross section is presented. The dashed line in graph c) corresponds to the dispersionless curve $\lambda(k) = \pi + 2\pi k/3$.

and plot the result in Fig. 3(d-f). While the cases $V = 0, 1$ yield the typical dispersive wave packet spreading, we find that for $V = \sqrt{4.8}$ exactly one third of the wave packet is propagating in a relativistic nondispersive manner to the right, leading to the effect of charge separation (see [13] for a detailed calculation of the charge separation value).

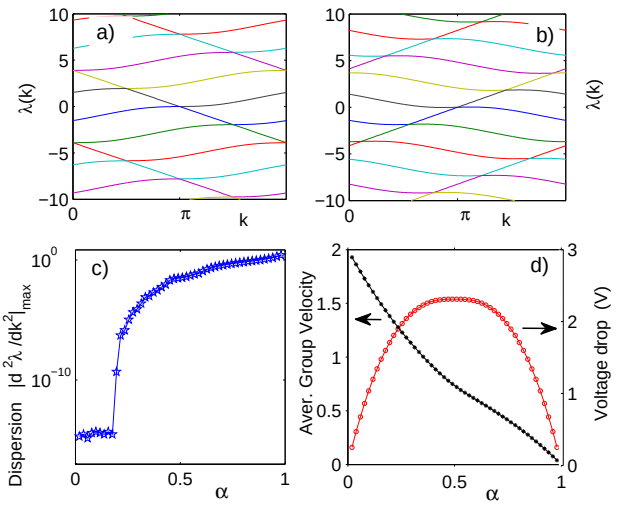

FIG. 4: Upper plots: Band structure for relative flux values $\alpha = 3/4$, $\alpha = 2/9$ and voltage drops $V = 1.8322$ (a) and $V = 0.8676$ (b). Lower plots: The α dependence of the largest dispersion $|\partial^2\lambda/\partial k^2|$ (c), of the averaged group velocity $|\langle\partial\lambda/\partial k|$ (black stars) and of the largest voltage drop value V_1 (red circles) (d) for the analyzed cases of charge separation in the gap closing regime. Note that only rational values of α are considered here.

For general rational relative flux values $\alpha = p/s$ one has to consider an $s \times s$ matrix $\hat{M}^{(s)}_{\alpha=p/s}$. Then the condition $Det\left(M^{(s)}_{\alpha=p/s}\right) = 0$ gives s real roots for $V = \pm|V|$.

The root with the largest absolute value will yield p/s fractional transport, which can be found either analytically or numerically. In the upper panel of Fig. 4 band structures for two different relative flux values $\alpha = 3/4$ and $\alpha = 2/9$ are shown in the gap closing regime ($V = 1.8322$ and $V = 0.8676$ respectively). Fractional transport with exactly 3/4 and 2/9, respectively, of the total charge is observed in numerical simulations. In the lower panel of Fig.4 we plot the largest dispersion $|\partial^2\lambda/\partial k^2|$ (c), and the averaged group velocity $|\langle\partial\lambda/\partial k|$ (d) for the analyzed cases of charge separation in the gap closing regime. While the dispersion is very small but nonzero for $\alpha \geq 1/6$, it vanishes for $\alpha < 1/6$. In the same limit of small α values the group velocities of the fractional charge tend to their largest values.

So far we considered charge separation for the largest root of voltage drop given by $Det\left(M^{(s)}_{\alpha=p/s}\right) = 0$. Interestingly, the other roots yield an even more complex charge separation scenario. For $\alpha = 1/11$ we examine the corresponding block matrix $M^{(11)}_{\alpha=1/11}$ with dimension 11×11. The gaps close when the condition $Det\left(M^{(11)}_{\alpha=1/11}\right) = 0$ is fulfilled which produces five nontrivial independent positive roots: $V_5 = 0.0869$, $V_4 = 0.2244$, $V_3 = 0.4135$, $V_2 = 0.6585$ and $V_1 = 0.9660$.

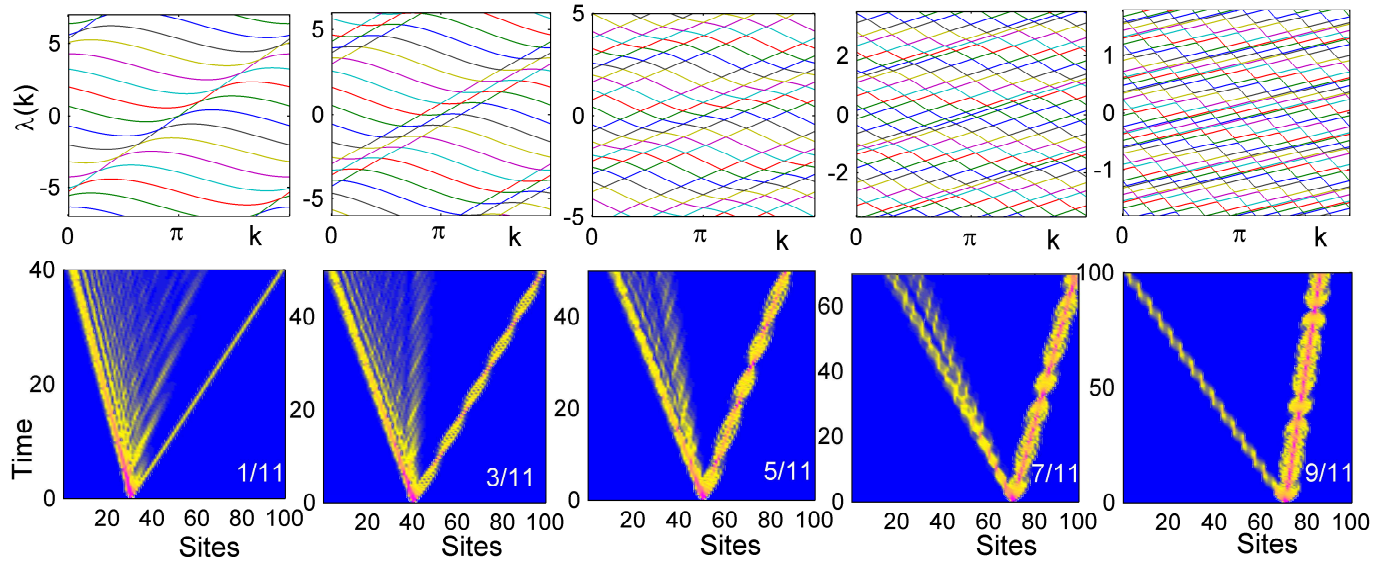

FIG. 5: Same as in Fig. 3 but with different parameters: the relative magnetic field flux is $\alpha = 1/11$ and the voltage drop values are the five roots of the equation $Det\left(\hat{M}^{(11)}_{\alpha=1/11}\right) = 0$, in particular $V = 0.9660,\ 0.6585,\ 0.4135,\ 0.2244,\ 0.0869$ (from left to right). Note different time scaling in lower panel. Corresponding video files representing charge dynamics in 2D lattice could be found in supplemental material.

The corresponding band structure (upper panel) and fractional charge dynamics (lower panel) with single site initial conditions are shown in Fig. 5. For the largest root $V = V_1$ a fraction of $1/11$ of the charge is separated and is propagating relativistically (see [13] for numerical evidence). This follows straight from the band structure, since only one of the eleven bands is yielding a positive nondispersive group velocity (see first column of Fig. 5). The dependence of this largest voltage drop V_1 on various rational values of α is shown in Fig.4 (d). We observe that in the limit of weak magnetic fields the corresponding voltage drop values tend to zero as well, however keeping the surprising feature of fractional relativistic transport.

For the other roots more bands are contributing to the fractional current, while still only one is completely gapless, as shown in Fig.5. Moreover, the nonzero gaps become much smaller, leading to almost relativistic charge separation in both directions (lower panels in Fig.5). The value of the charge fraction is now given by the number of the participating bands times the value of α. In our case of V_m nontrivial positive roots with $m = 1, 2, 3, 4, 5$ we find that the charge fraction is given by $(2m-1)\alpha$ (see [13] for numerical evidence).

The observed fractional charge transport is crucially linked to the orientation of the electric field. In our case it is directed along the diagonal of a square lattice. Consider instead an electric field orientation along a main axis of the square lattice. In that case the momentum k of motion perpendicular to the electric field will completely decouple from the magnetic flux. As a result the matrix $\hat{M}$ in Eq.(6) will not decouple anymore into two noninteracting blocks at a special value of k, since k will enter its diagonal part only. This will destroy the exact degeneracies which lead to fractional transport.

In summary, we demonstrate that a simple quadratic lattice is sufficient to obtain fractional charge separation of noninteracting electrons, or ultracold atomic gases, in the presence of magnetic fields, or synthetic gauge fields and a properly oriented and tuned DC bias. Such a charge separation can be potentially very useful for the preservation and engineering of entanglement in quantum systems.

[1] R.E. Prange, S.M. Girvin (Eds.), *The Quantum Hall Effect*, Springer (1990).
[2] P. G. Harper, Proc. Phys. Soc. A **68**, 874 (1955).
[3] T. Nakanishi, T. Ohtsuki, M. Saitoh, J. Phys. Soc. Jpn. **64**, 2092 (1995).
[4] H.N. Nazareno, P.E. de Brito, Phys. Rev. B **64**, 045112 (2001).
[5] A.R. Kolovsky, G. Mantica, Phys. Rev. B **86**, 054306 (2012).
[6] A.R. Kolovsky, I. Chesnokov, G. Mantica, Phys. Rev. E **86**, 041146 (2012).
[7] B.P. Anderson, M. Kasevich, Science **282**, 1686 (1998).
[8] M. Cristiani, O. Morsch, J. H. Müller, D. Ciampini, E. Arimondo, Phys. Rev. A **65**, 063612 (2002).
[9] J. Struck, C. Ölschläger, M. Weinberg, P. Hauke, J. Simonet, A. Eckardt, M. Lewenstein, K. Sengstock, P. Windpassinger, Phys. Rev. Lett. **108**, 225304 (2012).
[10] S. Longhi, M. Marangoni, M. Lobino, R. Ramponi, P. Laporta, E. Cianci, V. Foglietti Phys. Rev. Lett. **96**, 243901 (2006).
[11] M. Golshani, S. Weimann, Kh. Jafari, M. Khazaei Nezhad, A. Langari, A.R. Bahrampour, T. Eichelkraut, S.M. Mahdavi, A. Szameit, Phys. Rev. Lett. **113**, 123903 (2014).
[12] J. Vidal, R. Mosseri, B. Doucot, Phys. Rev. Lett, **81**, 5888 (1998).
[13] See Supplemental Material at **URL to be defined**.
[14] J. von Neumann and E. P. Wigner, Z.Physik **30**, 467 (1929).